

Evaluation of Dual Electrochemical Cell Design for Cerium-Vanadium Redox Flow Battery to Use Different Combination of Electrodes

Muthuraman Govindan, Ke He and Il-Shik Moon*

Dept. of Chemical Engineering, Sunchon National University, 255 Maegok Dong, Suncheon 540-742, Chonnam, Korea

*E-mail: ismoon@sunchon.ac.kr

Received: 3 June 2013 / Accepted: 30 June 2013 / Published: 1 August 2013

Dual electrochemical cells for various combinations of electrodes is developed and evaluated for the application of cerium-vanadium redox flow battery. By the evaluation of electrochemical oxidation/reduction with time for Ce and V using different individual electrode (Pt coated Ti, graphite, Pb, SS, and DSA) results demonstrate applicability of various combination of electrode pairs in Ce-V redox flow battery. Cyclic voltammetry results of Ce and V at different electrodes corroborate their redox property in methanesulfonic acid and sulfuric acid towards finding suitable electrode pairs. Single electrochemical cell allows only two different electrodes combination like Pt-Pt, Pt-graphite, graphite-graphite etc.. Dual electrochemical cell paved way to use four different electrodes combination such as DSA-Pt//graphite-graphite, Pt-graphite//Pb-SS etc. Charging and discharging rate of Ce and V demonstrated that the Pt-graphite of charging and Pb-SS for discharging is more suitable combination. At a given current density (85.7 mA cm^{-2} for charging, 14.3 mA cm^{-2} for discharging), the full three charge and discharge cycles at 4 hr duration is obtained with little decrease in further each cycle (120 min - 80 min). Under optimized flow rate 600 ml min^{-1} , 50° C , different area of electrode, the energy efficiency (85.4%), voltage efficiency (46.5%), and current efficiency (80.1%) were achieved using the dual electrochemical cell with different combination of electrodes. These indicate that the dual electrochemical cell with various combinations of electrodes is a promising candidate for Ce-V RFB applications.

Keywords: Ce-V redox flow battery, methanesulfonic acid, combination of electrodes, dual electrochemical cell.

1. INTRODUCTION

Although, electrical energy produced by thermal and hydro-electrical route [1,2], insufficient energy storage facility can lead to problems, such as high volatility and an increased burden on

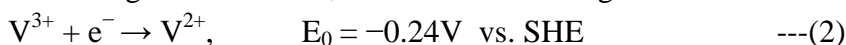
electricity distribution systems [3]. A right solvable support could be redox flow battery (RFB). A typical application of RFBs is load-leveling, which consists of storing energy during off-peak hours and releasing it when the demand raises [3,4]. RFB technology can also be used in combination with renewable power sources, such as photovoltaic cells [5] and wind turbines [6]. Due to the rapid growth of renewable energy and more advanced power generating sources, increasing attention has been given to the development of more advanced, reliable and safer redox flow batteries. A number of RFBs, such as iron–chromium [7], all vanadium [8], zinc–bromine [9], zinc–chlorine [10], polysulfide–bromine [11], zinc–ferricyanide [12], zinc–air [13], vanadium–cerium [14] and zinc–cerium [15] cells and soluble lead acid cells [16] have been developed.

Both vanadium [17] and cerium [18] are advantageous materials for energy storage due to the relatively large differences between their standard electrode potentials in aqueous media. Because of high standard reduction potential (1.56 V vs SHE), the $\text{Ce}^{3+}/\text{Ce}^{4+}$ redox couple [19-21] has been considered as the positive electrode reaction in cerium-vanadium battery. Combined redox potential of cerium-vanadium RFB (Ce-V RFB) has a standard reduction potential as follows:

At the positive electrode, the reaction on charge would be:



At the negative electrode, the reaction on charge would be:



To optimize the full Ce-V redox flow cell, an improved understanding of the effective oxidation/reduction of cerium and vanadium at electrode with suitable design is crucial among membrane [22] and electrolytes [23-25] etc. To date, very limited works have been published on charging/discharging studies for Ce-V RFB. Previous studies mainly focus on the redox behavior and charging/discharging of cerium half cell [14,26] using CV studies. In particular described about cerium redox behavior on various electrodes like Au, GC [27,28], PbO_2 [29,30], SnO_2 [31] and the reduction of Ce^{4+} at Pt, Au, Ir [32,33], and highly boron-doped conductive diamond electrodes [34]. Carbon plastic anode was used for Zn/Ce RFB system [35] for more stability of anode. Among these Ce half cell studies, carbon based electrodes follow quasi-reversible or nearly reversible redox process [27] towards cerium oxidation/reduction. It is well recognized that the highly reversible redox process gives only high energy efficiency [32]. However, carbon electrode may not be suitable for long time operation of Ce-V RFB due to dissolution of carbon particles during oxidation of Ce^{3+} using constant current method. In case of vanadium redox property, carbon based electrodes are more efficient [22]. Skyllas-Kazacos and coworkers have mentioned in their patent for all vanadium redox flow battery (VRFB) that different electrode combination can be used for two different redox couples like Ce-V, Ce-Zn and so on [36]. Using the idea of different combination of electrode, the two half cell or full cell charging/discharging behavior in Ce-V aims to explore. Till date no detailed studies on full cell Ce-V RFB with different combination of electrodes were published to our literature knowledge.

In this investigation, combinations of electrodes were attempted for charging (cerium oxidation/vanadium reduction) and discharging (cerium reduction/vanadium oxidation) electrochemical cell separately. For comparison, usual electrochemical cell with Pt-Pt as anode and cathode, charging and discharging respectively, was tested and compared. Additional studies such as cyclic voltammograms (CV), oxidation/reduction rate of $\text{Ce}^{3+}/\text{Ce}^{4+}$ and $\text{V}^{3+}/\text{V}^{2+}$, number of cycles, and

energy efficiency were carried out for confirmation. Further, anolyte 4 M MSA and catholyte 2 M sulfuric acid were used due to high solubility of 1.0 M Ce^{3+} and 1.0 M V^{3+} respectively.

2. EXPERIMENTAL

2.1. Preparation of electrolyte

Cerium(III) in methanesulfonate was prepared by mixing cerium(III) nitrate powder (DAEJUNG, Korea, 99.0 wt.%) with aqueous methanesulfonic acid (MSA) (DAEJUNG, Korea, 99.0 vol.%) to produce concentrations of 1 M Ce^{3+} in 4 M methanesulfonic acid. Vanadium (III) solution was prepared by electrochemical route [37] using VOSO_4 (Sigma–Aldrich, Japan, 97.0 wt.%) 2 M sulfuric acid (DC Chemical, Korea, 95.0 vol%).

2.2. Battery charge and discharge process

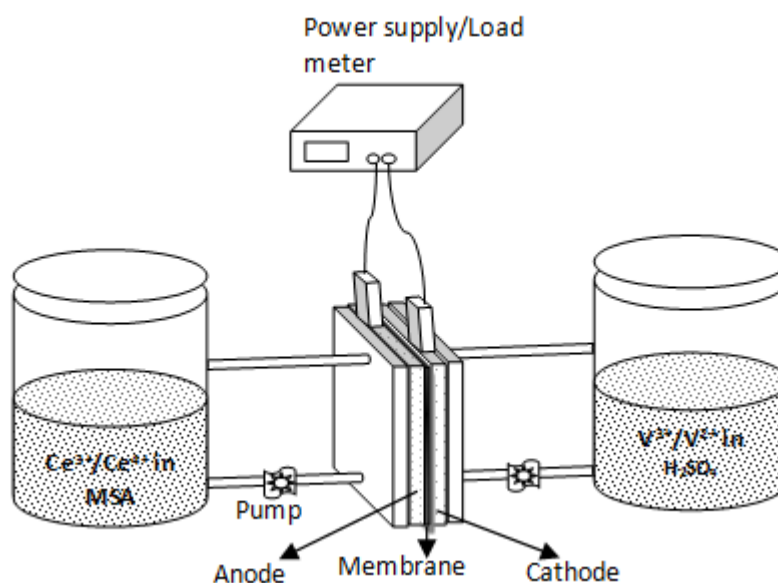


Figure 1. Schematic representation of conventional single electrochemical cell with power supply and load meter.

The conventional Ce-V cell for electrochemical oxidation of $\text{Ce}^{3+}/\text{Ce}^{4+}$ and reduction of $\text{V}^{3+}/\text{V}^{2+}$ were carried out in a divided, parallel plate flow cell as shown in Fig. 1. The cell consisted of a polyvinyl chloride (PVC) casing holding two flow channels, which contained the negative and positive electrodes, separated by a cation-conducting Nafion® membrane (DuPont, U.S.A., NF117/H⁺). Rubber silicon gaskets of 1.5 mm thickness were used between the compartments and membrane. The overall outer dimensions of the cell were 20 cm × 13 cm × 8 cm. The effective area (35 cm²) was 4.5 cm × 8 cm × 4 mm for each compartment. Different types of electrodes were

prepared and used in the experiments: the mesh type of Pt (Pt coated Ti), DSA (dimensionally stable anode (IrO₂ and RuO₂)), and Ti electrode and the punched hole type graphite, Pb, and stainless steel (SS) electrodes.

The volume of the positive electrolyte (anolyte) 100 ml (1 M Ce³⁺) in 4 M MSA and the negative electrolyte (catholyte) 100 ml (1 M V³⁺) in 2 M sulfuric acid were taken in separate containers. Each electrolyte was circulated through the cell at a flow rate between 300 to 1000 ml min⁻¹ from respective containers using a peristaltic and magnetic pumps (Cole-Parmer Instrument, USA and Pan Co.Ltd, Taiwan). The charge process of battery was carried out at constant applied current of 1.0 and 3.0 A by using a power supply (SWITCHING, Korea), and the discharge process of the battery was carried out at constant applied current of 0.5 A by using an electronic load meter (SL-300, UNICORN, USA). The current density reported in these experiments was calculated taking into account the actual working area of the anode (area that is exposed to solution). Voltage efficiency, current efficiency, and energy efficiency were calculated as reported in ref. [15]. All the battery system was worked under the room temperature conditions.

2.3. Determination of the concentration of Ce⁴⁺ and V²⁺ and analysis

The concentration of Ce⁴⁺ in MSA was determined via a colorimetric redox titration method [38-40]. The steps followed were: approximately 0.1 ml of Ce⁴⁺ containing solution taken through calibrated syringe from the anolyte storage container; the solution was then titrated with of 0.01M FeSO₄ solution (JUNSEI, Japan, 99.5 wt.%) and the concentration of Ce⁴⁺ was determined from the amount of Fe²⁺ required for the complete reduction of Ce⁴⁺ (yellow color) to Ce³⁺ (colorless).

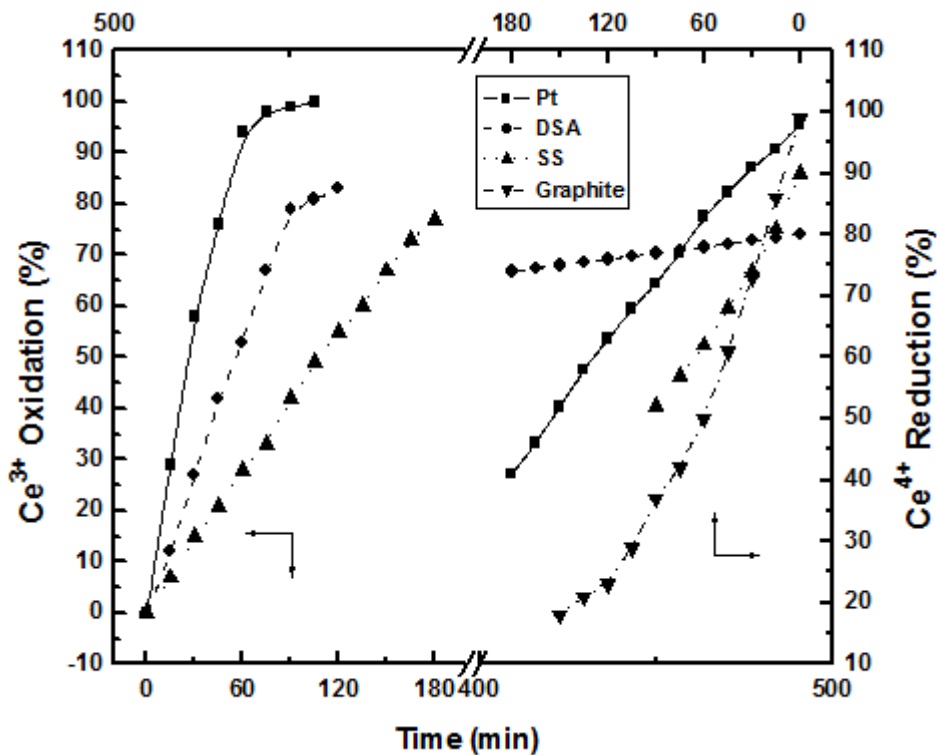
The concentration of V²⁺ in sulfuric acid was determined via a colorimetric oxidation titration method [41]. The steps followed were: approximately 0.1 ml of V²⁺ containing solution taken through syringe from the catholyte storage reservoir; the solution was then titrated with 0.01 M KMnO₄ solution (JUNSEI, Japan, 99.0 wt.%), and the solution color changed from purple color (V²⁺) to a green color (V³⁺) to a blue color (V⁴⁺) to a yellow color (V⁵⁺) and in the end to a red color due to the indicator. The concentration of V²⁺ was calculated by the volume changes of KMnO₄.

Cyclic Voltammetry experiments were carried out using PAR-290 instrument from USA. Pt, DSA, SS, Pb, and graphite with 1 cm² were working electrodes. Graphite rod (5 mm) served as counter electrode, and Ag/AgCl served as reference electrode, respectively. All the cyclic voltammetry experiments were carried out at 20 ± 1°C temperature.

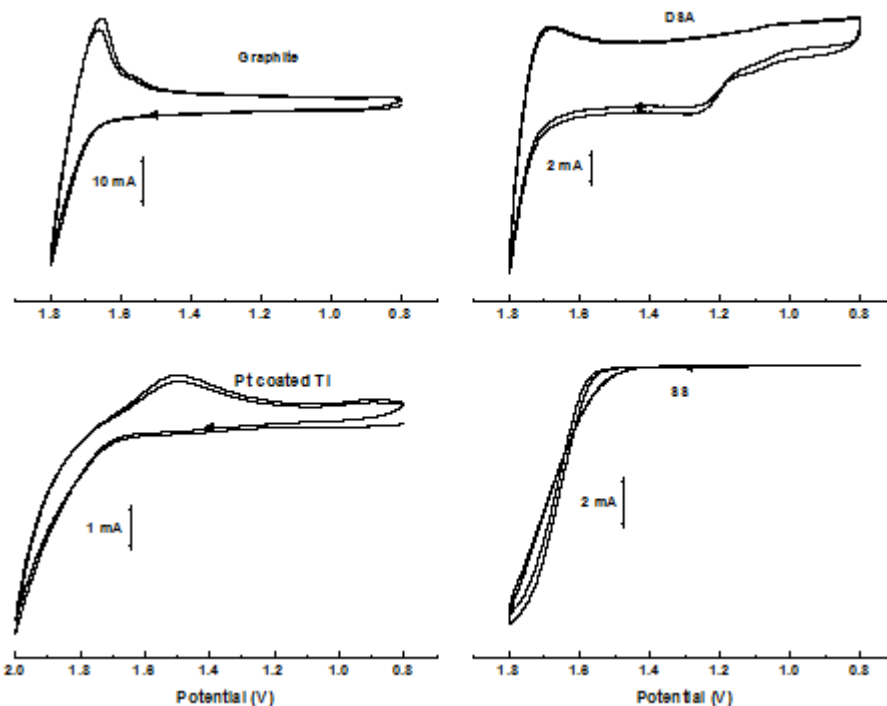
3. RESULTS AND DISCUSSION

3.1. Selection of electrodes through Ce³⁺ and V³⁺ oxidation/reduction process

Before going to RFB work, the redox properties of Ce³⁺ and V³⁺ are analyzed using both the galvanostatic and potentiostatic methods at different electrodes.



A

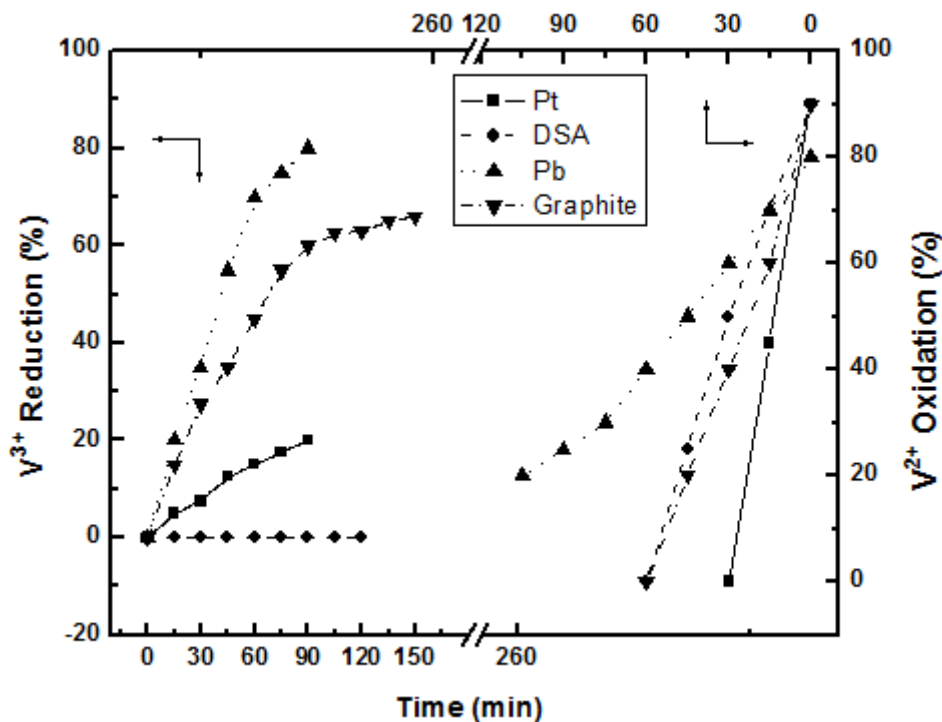


B

Figure 2. (A) Ce^{3+}/Ce^{4+} concentration variation on different electrodes in 4 M MSA. Conditions: current density 85.7 mA cm^{-2} ; Flow rate 300 ml min^{-1} ; Electrode area = 35 cm^2 ; Ce concentration = 1 M. (B) CV responses of Ce^{3+}/Ce^{4+} redox couple at different electrodes in 4 M MSA. Scan rate = 20 mV s^{-1} ; Concentration of cerium = 1 M.

Here, the electrolytes 1 M Ce³⁺ in 4 M MSA and 1 M V³⁺ in 2 M Sulfuric acid get energized by 3 A and 1 A using rectifier for cerium and vanadium oxidation/reduction by DSA and graphite electrodes respectively, the concentration of both Ce⁴⁺ and V³⁺ were calculated as mentioned in section 2.3, and depicted in supporting information Fig.SI 1(A&B). Only during input 3 A current shows almost 85% oxidation/reduction of cerium and reduction/oxidation of vanadium occurred within 2 hrs. For further investigation of cerium oxidation/reduction and vanadium reduction/oxidation using different electrodes were carried out at 3 A current and depicted in Fig.2A.

In the case of cerium, the oxidation rate is fast and higher at Pt electrode, i.e., exponentially increased 100 % within 60 min and remains constant. On the other hand, DSA and SS show nearly 80% oxidation efficiency that also reached by longer times, DSA (100 min) and SS (200 min). Unfortunately, graphite electrode shows no oxidation of Ce³⁺ (not able to measure) due to its particles dissolution to anolyte remember that applied current is 3 A. At the same time, cerium reduction occurs effectively, 85% to 16% during 120 min, on graphite, which is faster rate than other electrodes studied. The SS and Pt electrodes show nearly 45% and 40% reduction at 100 min and 200 min respectively. Almost no Ce⁴⁺ reduction occurred at DSA electrode. These results are well correlated with CV response. In order to compare with the real Ce-V RFB condition, the used electrodes were cut to needed size (1cm²) from the original (bigger) size and used as such without any treatment of electrode and electrolyte like N₂ gas purging for O₂ removal and dilution of the electrolytes. Fig.2B depicts the CV responses of Ce^{3+/4+} redox behaviors at different electrodes with a scan rate of 20 mV s⁻¹. In graphite electrode, there appears a steep raise in anodic current, where the oxidation peak of Ce³⁺ combined with oxygen evolution region, with defined reduction peak around 1.7 V that is reduction of Ce⁴⁺ is more favor, obtained only at graphite.



A

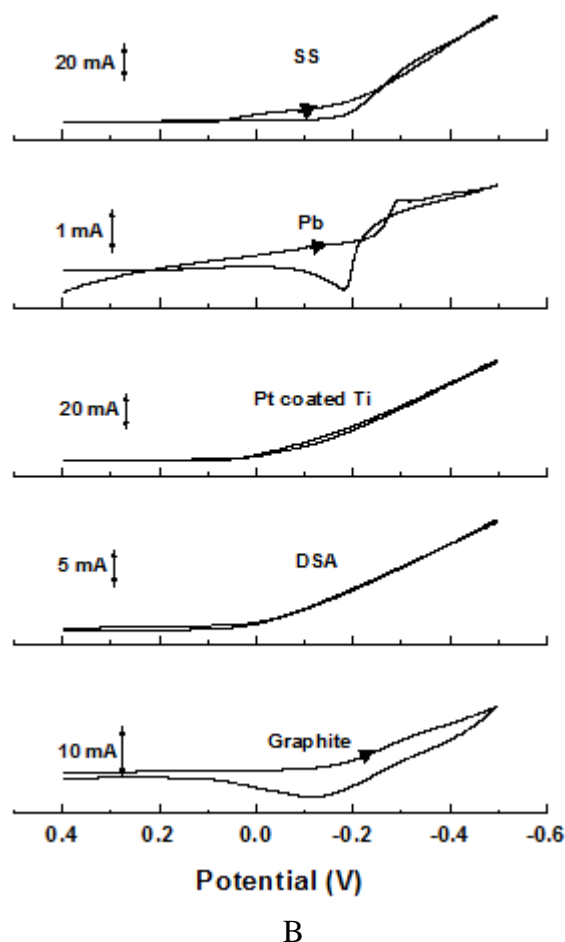


Figure 3. (A) Effect of V^{3+}/V^{2+} oxidation/reduction at various electrodes in 1 M H_2SO_4 . Conditions: current density= 85.7 mA cm^{-2} ; Flow rate= 300 ml min^{-1} ; Electrode area= 35 cm^2 ; Vanadium concentration 1 M.(B) CV responses of V^{3+}/V^{2+} redox couple at different electrodes in 1 M H_2SO_4 . Scan rate= 20 mV s^{-1} ; Concentration of Vanadium = 1 M.

Also DSA electrode shows cerium oxidation along with O_2 evolution with a less reduction peak current. Pt electrode shows reduction peak nearly at 1.5 V but SS electrode show no reduction peak at all, which well correlates with Ce^{3+} oxidation that Ce^{3+} and Ce^{4+} may not be oxidized and reduced at the same electrode through which it get oxidized or reduced.

Fig.3A depicts the oxidation/reduction of V^{3+}/V^{2+} at different electrodes for consideration of another half cell. Reduction of V^{3+} shows 80% within 60 min only at Pb electrode. Next, graphite electrode reached 65% around 100 min and Pt, and DSA show nearly no reduction of V^{3+} , especially DSA show 0% reduction. Perhaps while oxidation of V^{2+} , it reaches 0% within 30 min from 85% especially at Pt, graphite, and DSA electrodes. Nearly 20% oxidation efficiency was obtained in the case of SS electrode within 100 min, which tells that oxidation of V^{2+} is slow at SS than the other three electrodes. Fig.3B shows the CV response of V^{3+}/V^{2+} redox behavior at 20 mVs^{-1} . The graphite electrode shows a quasi-reversible redox peaks around -0.3 V and -0.12 V during forward and reverse scan, respectively. In the case of DSA and Pt, only steep raise in current with absence of

reduction/oxidation peak were observed at given conditions. Pb electrode shows a reduction peak around -0.3 V and an oxidation peak around -0.19 V with a curve crossing, which follows quasi reversible redox behavior with a new phase formation during reduction which is not the focus of the present work. Also, SS electrode shows no defined redox peak in V^{3+} reduction/ V^{2+} oxidation. All these explain that except graphite and Pb, no electrodes show reversible redox response for V^{3+}/V^{2+} couple. Again CV studies for V^{3+}/V^{2+} redox reaction prove that the same electrode which is used for reduction can't be used for oxidation.

3.2 Dual electrochemical cell for charging and discharging in Ce-V battery

As evidenced in previous section, no electrode is suitable for the both oxidation and reduction of the cerium and as well as vanadium at the same electrode, because of irreversible and quasi reversible behavior at all studied electrodes except graphite. But oxidation and reduction can be performed by choosing the two different electrodes especially one electrode for oxidation and another electrode for reduction of the same.

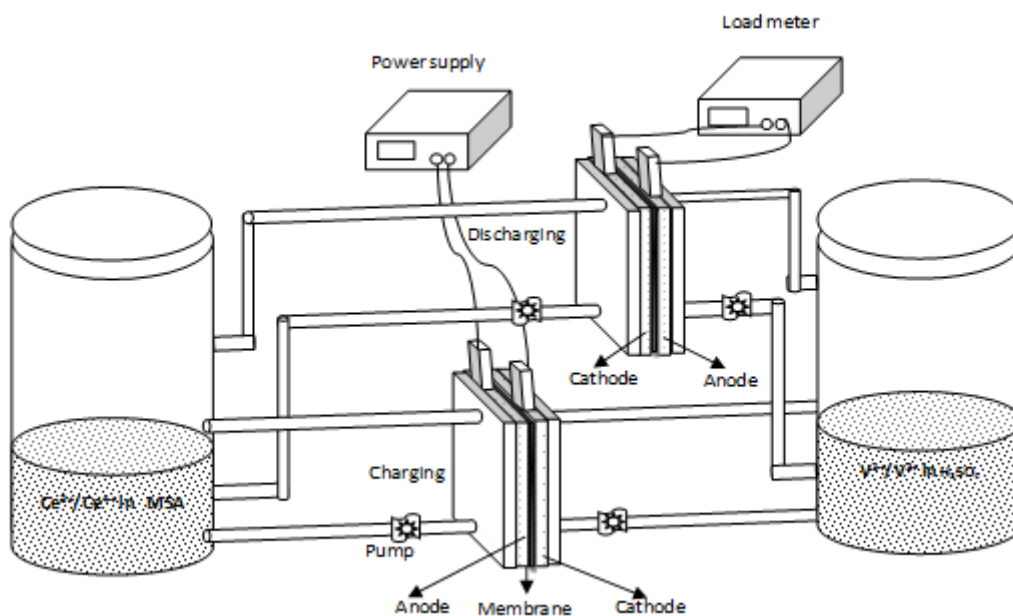


Figure 4. Pictorial representation of dual electrochemical cell for Ce-V RFB setup with possibilities for different combination of electrodes for charging and discharging steps.

With this idea, the dual electrochemical cell was introduced for charging and discharging separately, as shown in Fig.4. During charging Ce^{3+} oxidized to Ce^{4+} and V^{3+} reduced to V^{2+} using different combination of electrode, here Pt and Pb were used. While discharging Ce^{4+} reduced to Ce^{3+} and V^{2+} oxidized to V^{3+} by different pair of electrode, here three combinations were selected such as graphite-Pt, graphite-SS, and graphite-Ti. Using this idea, the experiments were carried out with different combination of electrode pairs to find out the more suitable electrode pairs for charging and

discharging in Ce-V RFB.

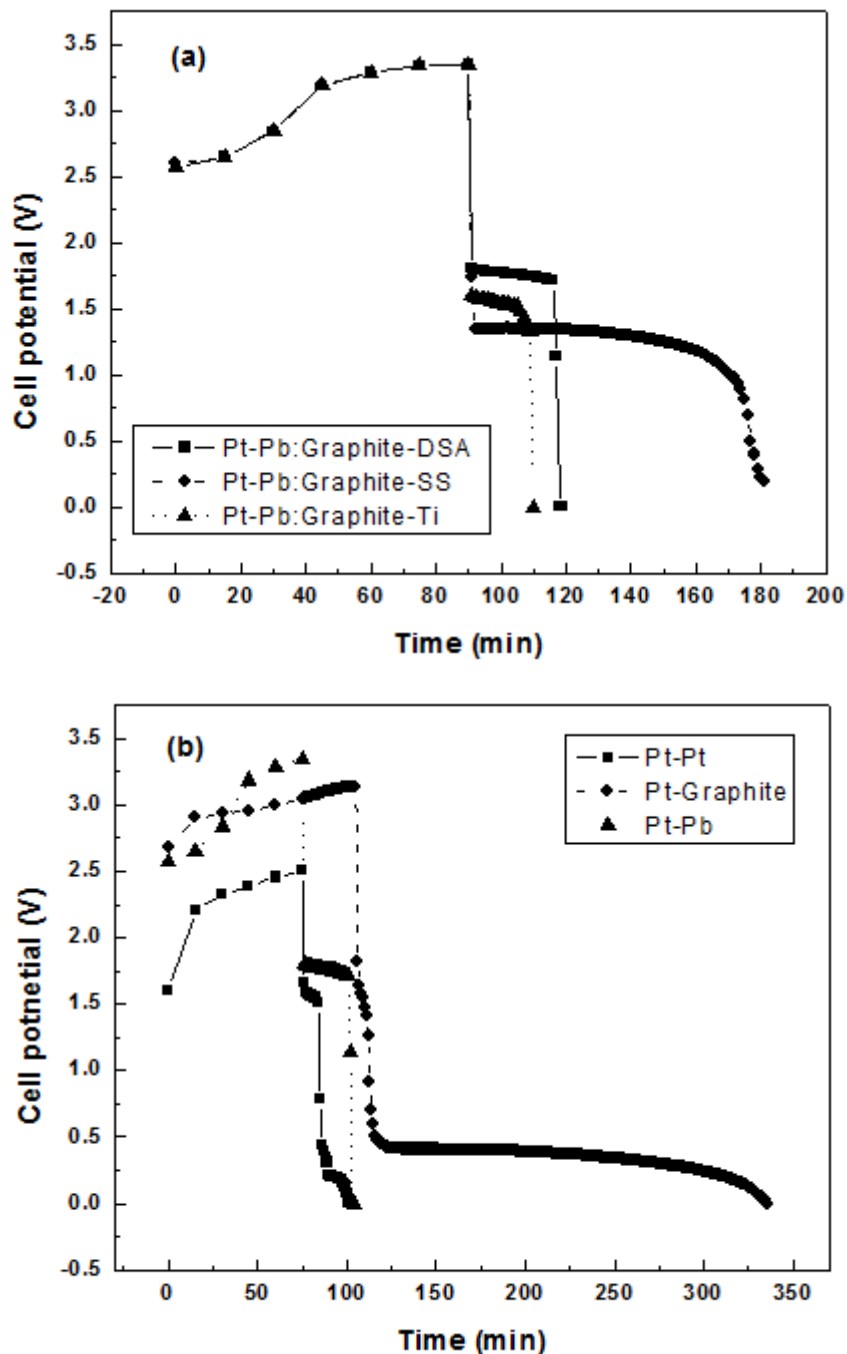


Figure 5. Charging/discharging response with time characteristics of a cerium-vanadium RFB equipped with different electrode pairs: (a) dual electrochemical setup with fixed electrodes Pt-Pb for charging and different pairs of electrodes for discharging steps; (b) conventional single electrochemical cell setup with different pair of electrodes for both charging and discharging steps. Electrolyte composition and operating conditions as in Fig. 2A and 3A. The discharging current density is 14.3 mA cm^{-2} .

Fig. 5a shows typical charge (Ce^{3+} oxidation- V^{3+} reduction) and discharge (Ce^{4+} reduction- V^{2+}

oxidation) potential limits with time at dual electrochemical cell using different combination of electrode pairs like Pt-Pb for charging and graphite-DSA, graphite-SS, graphite-Ti for discharging. It is found that the charging potential (upper limit) is reached to 3.3 V and remains almost the same up to 90 min then discharge process has initiated with different cell potential and ended depends on the electrode pairs. There appears no change in charging time, 90 min, due to use of only Pt-Pb electrode pair. If look at during discharging process in separate electrochemical cell, discharging time varies depends on the electrode pairs. Graphite-SS electrode pair shows complete discharge that occurred at 180 min. At the same time, the discharge cell electrode pair with graphite-DSA and graphite-Ti shows complete discharge within 30 min, which tells these two pair of electrodes is not suitable for discharging process in Ce-V RFB cell. The graphite-SS electrodes pair shows current and energy efficiency are 66% and 28%, shown in Table 1, which are low for practical application concerned. Additional curious point that found here is cell potential limits, remember that charging current is 3 A and discharging current is 0.5 A. The upper limits reached to 3.5 V and lower limit reached 0.5 V. It is known that the oxidation/reduction potential mainly varies with electrode, electrolytes, and applied current [42]. In present case at given conditions, as in Fig.SI1, the cell potential is reduced with decrease the applied current. It is known that the higher cell voltage minimize the energy efficiency due to water splitting [43]. To get high oxidation/reduction rate of cerium and vanadium and real application process, higher applied current is inevitable in this present case and experimental condition.

It is noting worthy that a few publications only published about Ce-V RFB there also focused half cell voltage especially for cerium charging/discharging process, where they applied 300 mA for charging and discharging with the half cell voltage of about 1.8 V [14]. Ludek et al., found that 2 A applied current for Ce(III) oxidation at carbon felt electrode showed 3 V [26]. Very recently charging/discharging full cell potential of Ce-Zn RFB was observed between the limits of 2.5 V to 0.5 V with the applied current of 300 mA [25]. These published result's cell voltage is well correlate with the present results that if reduce the applied current the cell potential is getting decreased. As mentioned above, we believed that there is some current loss in this high applied current but it can be rectified under optimized conditions. For comparison, the common single electrochemical cell was employed with different pair of electrodes. Remember that oxidation/reduction of cerium and vanadium employed at the same pair of electrodes. Fig.5b depicts the charge and discharge process at common electrochemical cell with different pair of electrodes. First, Pt-Pt pair of electrode shows completely charged around 60 min with the cell voltage of 2.5 V and the discharge time is six time reduced (10 min), which is very low.

The similar trend is observed for Pt-Pb pair of electrodes with little higher cell voltage (3.3 V for charging and 1.8 V for discharging). In the case of Pt-graphite pair of electrode, the time taken for charging is around 120 min with 3.2 cell voltage of 3.2 V and discharging time is very long, i.e., nearly 230 min, with 0.5 cell voltage.

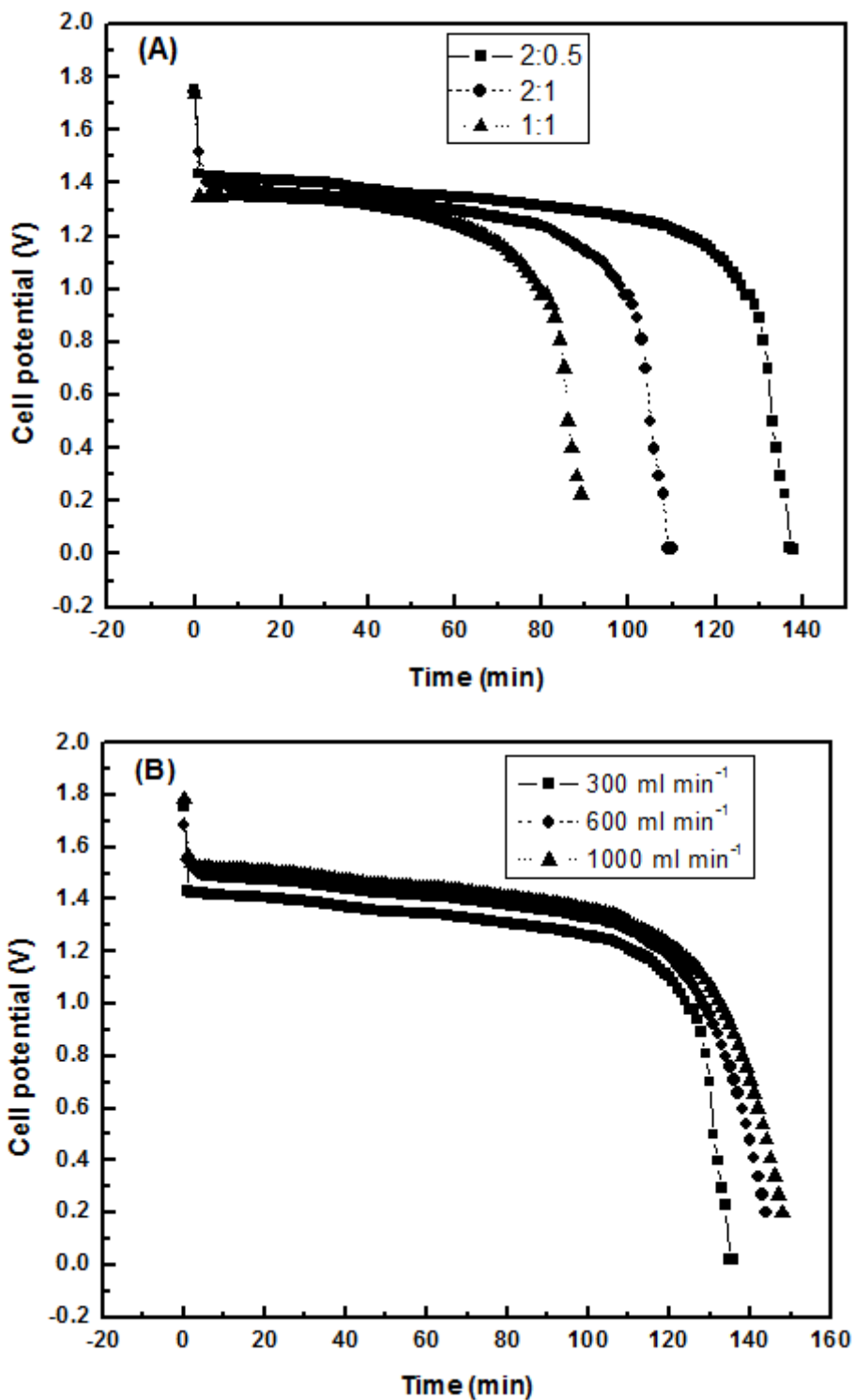


Figure 6. (A) Effect of electrode ratio on discharging response with time for Ce-V RFB at graphite-SS electrode pair: (a) 1:1; (b) 2:1, (c) 2:0.5. Electrolyte composition and operating conditions as in Fig. 2A and 3A. The discharging current density is 14.3 mA cm^{-2} . (B) Variation of liquid flow rate on discharging response with time for Ce-V RFB at graphite-SS electrode pair: (a) 300 ml min^{-1} (b) 600 ml min^{-1} (c) 1000 ml min^{-1} . Electrolyte composition as in Fig. 2A. Electrode ratio of graphite and SS is 2:0.5. The discharging current density is 14.3 mA cm^{-2} .

Table 1. Comparative energy efficiency obtained using conventional and dual electrochemical cell with different combination of electrodes

Electrodes Pair	Current Efficiency %	Voltage Efficiency %	Energy Efficiency %
Conventional cell			
Pt-Pt	16.7	21.0	3.5
Pt-Graphite	12.1	21.9	2.7
Pt-Pb	26.7	29.3	7.8
Dual cell			
Pt-Pb:Graphite-Pt	12.1	41.9	6.9
Pt-Pb:Graphite-SS	66.7	40.2	28.6
Pt-Pb:Graphite-Ti	6.7	42.3	3.1
Dual cell Under optimized conditions: Liquid flow rate=600 ml min ⁻¹ ; Graphite-SS electrode ratio=2:0.5; temperature = 50° C			
Pt-Pb:Graphite-SS	85.4	46.5	80.1

Among these three pairs of electrode Pt-Pb electrodes pair shows (Table 1) higher energy efficiency (7.8 %), which is 4 times lower than the energy obtained from dual electrochemical cell with the combination of electrode like Pt-Pb (charging) and graphite-SS (discharging). With the 28% energy efficiency, the present dual electrochemical cell with different combination of electrodes may not meet the real application. For reaching the real standard, the discharging cell performance planned to focus by changing the parameters like liquid flow rate, electrode size variation and experimental temperature. According to Fig.2A & 3A, Ce⁴⁺ reduction at graphite is less and V²⁺ oxidation is faster at SS. Basing on this result, the experiments constructed with different electrode sizes such as 2 times increased the electrode area of graphite by adding one more electrode parallel and SS electrode area reduced to half by masking epoxy resin. The obtained results are depicted in Fig.6A. There appears the discharging time is increased with increasing graphite electrode ratio against SS electrode. During optimization of liquid flow rate, also found extended discharging time at higher liquid flow rate as shown in Fig.6B. The discharging time varies from 130 min to 155 mins upon increasing the flow rate from 300 to 1000 ml min⁻¹. Unfortunately, there is no increase in discharge time upon increasing temperature from 20° C and 50° C (results not shown). Under these optimized conditions, the dual electrochemical cell with different combination of electrodes shows highly improved energy efficiency (80.1 %), current efficiency (85.4 %) and voltage efficiency (46.5 %). The less in voltage efficiency may be due to different electrode on oxidation/reduction of Ce-V.

The applicability of the dual electrochemical cell was further employed to check for recharge ability. Fig. 7 shows three consecutive charge and discharge cycles of Ce-V RFB using dual electrochemical cell. In the first cycle, the charge and discharge process take place 50 and 130 min respectively. In the third cycle, the same process reduces only to 30 and 70 min respectively, which explains the recyclability performance. We believe that the dual electrochemical cell with combination of electrodes will be a new trend in Ce-V RFB. Further work is being carried out to meet the real application.

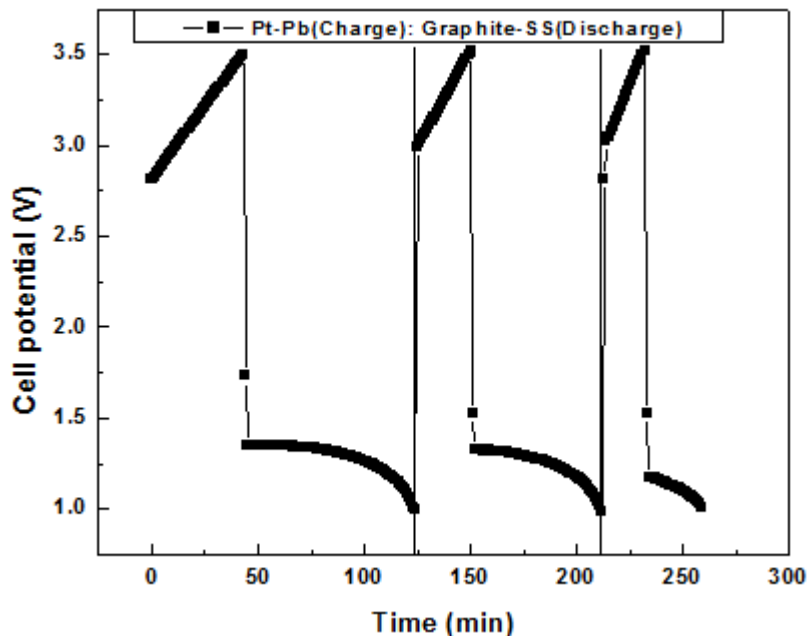


Figure 7. Three consecutive charging/discharging cycles of a Ce-V RFB at dual electrochemical cell. Electrolyte compositions and operating conditions were the same as in Fig. 2A. The charging and discharging current density is 85.7 and 14.3 mA cm⁻².

4. CONCLUSIONS

The newly developed dual electrochemical cell combined with suitably changeable electrode is evaluated successfully as Ce-V RFB. It is worth noting that the oxidation/reduction rate of cerium and vanadium at different pair of electrodes evidenced that no electrode was obeying redox performance of each component except graphite. The CV experiments once again confirm the irreversibility of cerium and vanadium at Pt, SS, Pb, and DSA electrodes. As a first attempt when compared to the conventional electrochemical cell, the dual electrochemical cell improves the energy efficiency 4 times (28.6%) at current densities of 85.7 and 14.3 mA cm⁻² in RFB system. Under optimized conditions, the energy efficiency increased to 80.1 %, current efficiency to 85.4%, and voltage efficiency to 46.5%. Also the number of cycle results confirms the feasibility of dual electrochemical cell to RFB system. In total, the dual electrochemical cell design is promising for multi electrolytes and electrode for RFB system.

ACKNOWLEDGEMENTS

This work was supported by several funding agencies: the Korea Ministry of Environment as "The Eco-technopia 21 project", the Korea Research Foundation Grant funded by the Korean Government (MOEHRD, KRF-2007-D00001), and the Korea Research Foundation and the Korean Federation of Science and Technology Society Grant funded by the Korean Government (MOEHRD, Basic Research Promotion Fund).

References

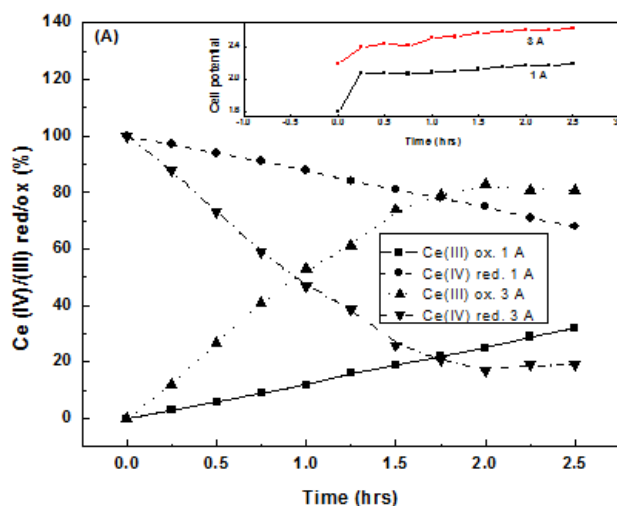
1. The Electricity Advisory Committee, Bottling Electricity: Storage as a Strategic Tool for Managing Variability and Capacity Concerns in the Modern grid - A report by The Electricity

- Advisory Committee, December (2008). <http://www.oe.energy.gov/DocumentsandMedia/final-energy-storage-12-16-08.pdf> Accessed on 01 March (2013).
2. N. Tokuda, T. Kanno, T. Hara, T. Shigematsu, Y. Tsutsui, A. Ikeuchi, T. Itou and T. Kumamoto, *SEI Tech. Rev.* 50 (1998) 88–94.
 3. J. Makansi and J. Abboud, *Energy Storage Council White Paper* (2002).
 4. C. Ponce de Leon, A. Frias-Ferrer, J. Gonzalez-Garcia, D.A. Szanto and F.C. Walsh, *J. Power Sources* 160 (2006) 716–732.
 5. L. Joerissen, J. Garche, C. Fabjan and G. Tomazic, *J. Power Sources* 127 (2004) 98–104.
 6. K.L. Huang, X.G. Lia, S.Q. Liu, N. Tan and L.Q. Chen, *Renewable Energy* 33 (2008) 186–192.
 7. M. Yoshitake, M. Takabatake, O. Hamamoto, T. Hiramatu and S. Kondo, *J. Proc. Electrochem. Soc.* 266 (1988) 11–88.
 8. M. Rychcik and M. Skyllas-Kazacos, *J. Power Sources* 22 (1988) 59–67.
 9. R.F. Koontz and R.D. Lucero, *Handbook of batteries*, vol. 39, 1–22 (2000).
 10. P.C. Butler, P.A. Eidler, P.G. Grimes, S.E. Klassen and R.C. Miles, *Handbook of Batteries*, vol. 39, 3rd ed., McGraw Hill (2001).
 11. F.C. Walsh, *J. Pure Appl. Chem.* 73 (2001) 1819–1837.
 12. L.W. Hruska and R.F. Savinell, *J. Electrochem. Soc.* 128 (1981) 18–25.
 13. Y.H. Wen, J. Cheng, S.Q. Ning and Y.S. Yang, *J. Power Sources* 188 (2009) 301–307.
 14. B. Fang, S. Iwasa, Y. Wei, T. Arai and M. Kumagai, *Electrochim. Acta* 47 (2002) 3971–3976.
 15. R.L. Clarke, B.J. Dougherty, S. Harrison, P.J. Millington and S. Mohanta, US 2004/0202925 A1, *Cerium Batteries* (2004).
 16. D. Pletcher and R. Wills, *J. Power Sources* 149 (2005) 96–102.
 17. X. Xia, H. Liu and Y. Liu, *J. Electrochem. Soc.* 149 (2002) A426–A430.
 18. P.K. Leung, C. Ponce de Leon, C.T.J. Low and F.C. Walsh, *Electrochim. Acta* 56 (2011) 2145–2153.
 19. Y. Wei, B. Fang and M. Kumagai, *J. Appl. Electrochem.*, 35 (2005) 561–566.
 20. P. Trinidad, C. Ponce de Leon and F.C. Walsh, *J. Environ. Manage.* 88 (2008) 1417–1425.
 21. Y. Liu, X. Xia and H. Liu, *J. Power Sources* 130 (2004) 299–305.
 22. W. Wang, Q. Luo, B. Li, X. Wei, L. Li and Z. Yang, *Adv. Funct. Mater.* 23 (2013) 970–986.
 23. D. Pletcher, H.T. Zhou, G. Kear, C.T.J. Low, F.C. Walsh and R.G.A. Wills, *J. Power Sources* 180 (2008) 630–634.
 24. G.-Y. Lee, H.-Y. Sun, J.-W. Park and S.U. Son, *Organic electrolyte solution and redox flow battery including the same*: EP 2355223 A1 (2011).
 25. Z. Xie, F. Xiong and D. Zhou, *Energy Fuels* 25 (2013) 2399–2404.
 26. J. Ludek, W. Yuezhou and M. Kumagai, *J. Rare Earths* 24 (2006) 257 - 263
 27. E. Bishop and P. Cofve, *Analyst* 106 (1981) 316–322.
 28. A. Paulenova, S.E. Creager, J.D. Navratil and Y. Wei, *J. Power Sources* 109 (2002) 431–438.
 29. T.H. Randle and A.T. Kuhn, *Aust. J. Chem.* 42 (1989) 229–242.
 30. T.H. Randle and A.T. Kuhn, *Aust. J. Chem.* 42 (1989) 1527–1545.
 31. R. Kotz, S. Stucki and B. Carcer, *J. Appl. Electrochem.* 21 (1991) 14–20
 32. T.H. Randle and A.T. Kuhn, *J. Chem. Soc., Faraday Trans. I* 79 (1983) 1741–1756.
 33. S. Ferro and A.D. Battisti, *Phys. Chem. Chem. Phys.* 4 (2002) 1915–1920.
 34. Y. Meada, K. Sato and R. Ramaraj, *Electrochim. Acta* 44 (1999) 3441–3449.
 35. R.L. Clarke, B.J. Dougherty, S. Harrison and J.P. Millington, *Battery with bifunctional electrolyte. United States Patent Application, International publication number: WO 2004/095602 A2*, November 4 (2004).
 36. M. Skyllas-Kazacos, M. Kazacos and R. McDermott, *Vanadium charging cell and vanadium dual battery system*, Patent Appl. No. PCT/AU88/00473, December (1988).
 37. E. Kjeang, B.T. Proctor, A.G. Brolo, D.A. Harrington, N. Djilali and D. Sinton, *Electrochim. Acta*, 52 (2007) 4942–4946.

38. P. Patnaik, *Dean's Analytical Chemistry Handbook*, 2nd ed., McGraw-Hill, (2004).
39. I.M. Kolthoff and E.B. Sandell, *Texture of Quantitative Inorganic Analysis*, 3rd ed. The Macmillan Company, 463–481 (1956).
40. A.I. Vogel, *Textbook of Quantitative Inorganic Analysis*, 5th ed. Wiley, New York (1989)
41. K.L. Chawla and J.P. Tandon, *Talanta*, 12 (1965) 665–669.
42. A.J. Bard and L.R. Faulkner, *Electrochemical Methods: Fundamental and Applications*, first ed., John Wiley & Sons, New York (1980).
43. E. Bishop and P. Cofre, *Analyst* 106 (1981) 316-322.

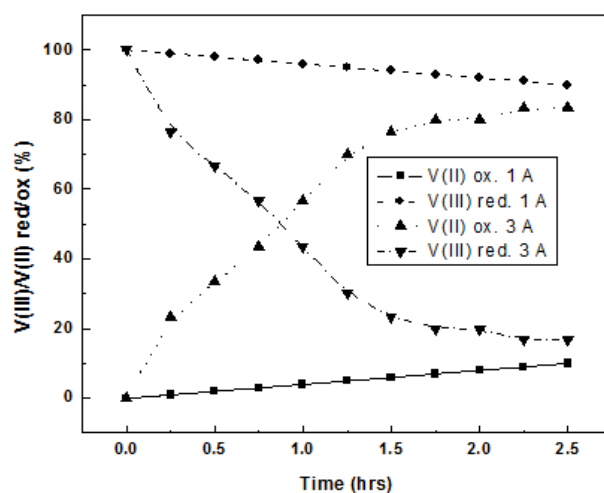
SUPPORTING INFORMATION:

Fig.SI 1A



(A) $\text{Ce}^{3+}/\text{Ce}^{4+}$ concentration variation on different applied current in 4 M MSA at DSA electrode. Conditions: Flow rate 300 ml min^{-1} ; Electrode area = 35 cm^2 ; Ce concentration = 1 M. Inset figure shows cell potential variation with different applied current.

Fig.SI 1(B)



(B) $\text{V}^{3+}/\text{V}^{2+}$ concentration variation on different applied current (mentioned in the figure) in 1 M H_2SO_4 at graphite electrode. Conditions: Flow rate 300 ml min^{-1} ; Electrode area = 35 cm^2 ; Ce concentration = 1 M.